

Analysis of Dry and Wet Water Vapor Imagery Characteristics of a Strong Precipitation Process in Bayannaer City

Lingdong Sun^{1,2}, Jianwei Wen²

¹Bayannaer Meteorological Bureau. Linhe, Inner Mongolia, China, 015000

²Inner Mongolia Autonomous Region Meteorological Data Center, Hohhot, Inner Mongolia, China, 01000

Abstract: Diagnostic analysis of a strong precipitation process from the aspects of FY2E Satellite Water Vapor Imagery of dry and wet characteristics occurred on 14~17 April 2014 in Inner Mongolia of Bayannaer City, by using the conventional meteorological data from MICAPS. The results showed that: (1) The vapour band located in the deep wet area has a θ se ridge axis and the shape and size of vapour band is consistent with it. The maintenance of high θ se ridge axis at low layer shows warm air from low latitude which is conducive to the atmospheric stratification instability appear below the vapour band. Due to the existence of upper troposphere dry intrusion, internal θ se in vapour band is higher than the outside 5 ~ 10 Centigrade. (2) The vapor zone has obvious vertical ascending motion in this precipitation process. The location of vapor band has a good relationship with the positive divergence, negative vorticity and vertical velocity of ascending motion area. On the west side of the boundary and negative vorticity in the upper troposphere are nearly parallel, dark area position with very strong positive vorticity.

Keywords: Water vapor image; Dry and wet characteristics; Vapour band; Strong precipitation

1. Introduction

Introduction Bayannur City is located in the the Inner Mongolian Plateau deep in the interior. The annual precipitation distribution gradually increases from northwest to southeast, from less than 80 mm in the northwest to 260 mm in the southeast, with a difference of nearly 180 mm. The annual precipitation of Hailisu, Wuhou Banner, Qiandamen, Hanghou Banner, Dengkou and Linhe in the west is only 127~146 mm; The eastern regions of Ulan, Wuzhong Banner, Wuqian Banner, and Dashetai have relatively more precipitation in the city, with rainfall ranging from 186 to 225mm; In sharp contrast to the precipitation, the evaporation of Bayannur City is 1992~2351mm in the south of Yinshan; It is 2435~3305mm in the north. The ratio of evaporation to precipitation is 9.6 times in Dashetai, 11.1~17.0 times in Hetao, and 12.2~26.1 times in Houshan. Bayannur City has an annual sunshine duration of 3131-3332 hours, with a sunshine percentage of 71% to 75%, making it a region with abundant sunshine in China. The spring (March May) precipitation in the city is distributed between 15.1-24.4mm, and the precipitation increases from northwest to southeast regionally. In the 30 years from 1971 to 2000, there were 8 years with an average precipitation of ≤ 10 mm in the city, which were 1971, 1974, 1978, 1986, 1989, 1993, 1995, and 2000, accounting for 26.7%; The years with precipitation ≥ 25 mm are 6 years, namely 1985, 1988, 1990, 1991, 1992, and 1998, accounting for 20%. Up to 20 years, accounting for 66.7%, have been less than the city's average, indicating that less spring rain and heavy drought are the biggest characteristics of spring precipitation in Bayannur City. From the night of April 14 to the night of April 16, 2014, most of Bayannur City experienced light to moderate rain. Among the 127 rainfall stations in Bayannur City, 3 stations were greater than 20mm, and 84 stations were greater than 10mm. The maximum precipitation occurred in the Shahai Xinsheng area of Hanghou Banner, reaching 27.2 mm. This precipitation process occurred in April (spring), and the cumulative precipitation level of this process reached the standard of strong precipitation in the local area. Due to the three-dimensional spatial structure of the atmosphere, forecasters not only focus on weather systems in the middle and lower troposphere, but also do not overlook systems in the middle and upper troposphere. Due to the ability of water vapor images to effectively reflect the weather system in the upper and middle troposphere. The important features of water vapor images are dry zone, wet zone, and dry wet boundary. The dark gray to nearly black areas on the image are

generally dry areas, while areas with medium gray to white bright tones are generally wet areas. Dry and wet areas correspond to the sinking and rising motion areas at the weather scale. The changes in wet and dry boundaries on water vapor images have clear indicative significance for the development of weather systems (Yang Jun et al., 2012). In recent years, many meteorological scientists and technicians, from the formation mechanism of rainstorm to the theoretical methods of monitoring and forecasting, have conducted in-depth discussions on the generation of rainstorm in different regions, and obtained many valuable achievements, such as Tao Shiyan systematically summarized the synoptic scale and mesoscale characteristics of the occurrence and development of rainstorm in China; Ding Yihui^[3] systematically reviewed the progress of rainstorm and mesoscale meteorology; Hou Ruiqin et al.^[4] carried out helicity diagnostic analysis on the 700 hPa shear line vortex related to the "98.7" extremely heavy rainstorm process. However, there is limited analysis of precipitation processes in terms of the characteristics of satellite water vapor images. As Bayannur City is located in the the Inner Mongolian Plateau deep in the interior, the time and space density of observation data is low, so the application of satellite data is particularly important for local weather forecasting.

This article uses MICAPS conventional meteorological observation data and FY2E satellite data, from the perspective of dry and wet characteristics of satellite water vapor images, combined with analysis methods such as weather dynamics and meteorological satellite science, to analyze the heavy precipitation weather process that occurred in Bayannur City from April 14 to 17, 2014, and to find the changes in dry and wet characteristics on water vapor images, improving the application level of satellite water vapor images in heavy precipitation weather analysis and prediction by forecasters.

2. Current situation in the upper troposphere

A lot of research shows that , rainstorm, severe convection and other weather are closely related to the circulation in the upper troposphere. From the water vapor image of the FY2E meteorological satellite at 20:00 on April 15, 2014, combined with the 300hPa potential height field and wind field (Figure 1a), it can be seen that the middle and high dimensions of the Eurasian continent are in a west low to east high pattern. The large low vortex extends from the eastern part of Lake Balkhash to the southern part of Xinjiang, and the area from Mongolia to Hetao is a high ridge area. Bayannur City is controlled by this high pressure ridge, and the ridge line is in a northwest southeast direction. Affected by the eastward movement of the rift trough at the bottom of the low vortex, the upstream Hexi Corridor The western part of Alxa League has a consistent southwest airflow, and due to the strong divergence zone in front of the trough, it appears as a relatively uniform large wet area on satellite cloud images. As the high-altitude trough slowly moved eastward, by 08:00 on the 16th (Figure 1b), Bayannur City was controlled by a large cloud system in front of the high-altitude trough, which was distributed in a sheet-like north-south direction and was white and bright in color. Due to the obvious divergent airflow over Bayannur City, it is conducive to low-level convergence and generates strong upward motion, resulting in heavy precipitation. There is an arc-shaped dark boundary from Mongolia to the Alashan League, indicating that there is cold air flowing south from the north. From the above analysis, it can be seen that the dry and wet characteristics on the water vapor image are obvious.

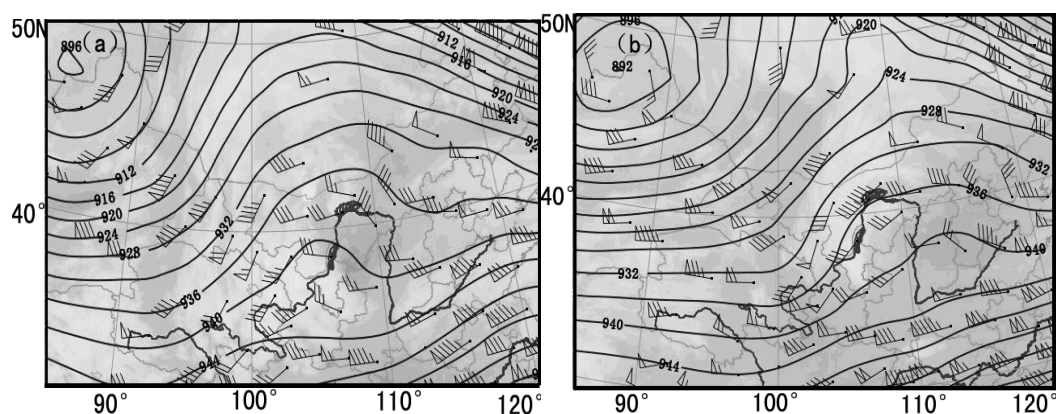


Figure 1: Superposition map of water vapor image and cloud induced wind of FY2E meteorological satellite at 20:00 (a) on the 15th and 08:00 (b) on the 16th (contour line is 300hPa potential height field, unit: gpm).

3. Dry and wet features on water vapor images

3.1. Wet zone characteristics

According to the continuous evolution of water vapor images from April 14 to 16, 2014, a nearly north-south distribution of water vapor is maintained from Mongolia to the Hetao region. The brightness on the water vapor belt is non-uniformly distributed, and the western boundary of the cloud body is clear. The eastern boundary has a filamentous cloud plume distribution, indicating strong divergence over the water vapor belt. There is a power point on the southwest side of the water vapor belt, and the gray scale of the power point gradually deepens and moves from southwest to northeast. The shape also evolved from a strip to a narrow strip, indicating a dry intrusion during this precipitation process.

The energy front zone is usually represented by the dense band of θ_{se} , As the unstable potential of atmospheric stratification is represented by the vertical distribution of θ_{se} , searching for low altitude θ_{se} ridge axis can determine the obvious unstable region of atmospheric stratification, and analysis θ_{se} The relationship between θ_{se} and water vapor bands can determine the environmental conditions conducive to the formation and development of mesoscale convective systems (MCS). During the precipitation process (at 08:00 on April 16th), it can be seen from the superposition of the water vapor image and the 850hPa pseudo equivalent potential temperature (Figure 3a). The dense zone of θ_{se} is located in the southern part of Mongolia to the southeastern part of Alxa League, indicating that this is the intersection of dry (cold) air from the north and humid (warm) air from the south. During this precipitation process, the range and shape of the water vapor belt were almost parallel to the ridge axis of 850hPa, indicating that this water vapor belt is a warm and humid conveyor belt^[10-13]. The Western Boundary of the Water Vapor Belt and θ_{se} The strong gradient band of θ_{se} is nearly parallel. Based on the above analysis, during this precipitation process, there is a θ_{se} ridge axis, the shape and range of the SE ridge axis are basically consistent with the water vapor belt, indicating that the area where the water vapor belt is located is a deep wet zone. The maintenance of the low θ_{se} ridge axis indicates that warm and humid airflow from low latitudes appears below the water vapor belt, which is conducive to the instability of atmospheric stratification; During this precipitation process, due to the presence of dry intrusion in the upper and middle troposphere, θ_{se} is 5-10°C higher than the outside.

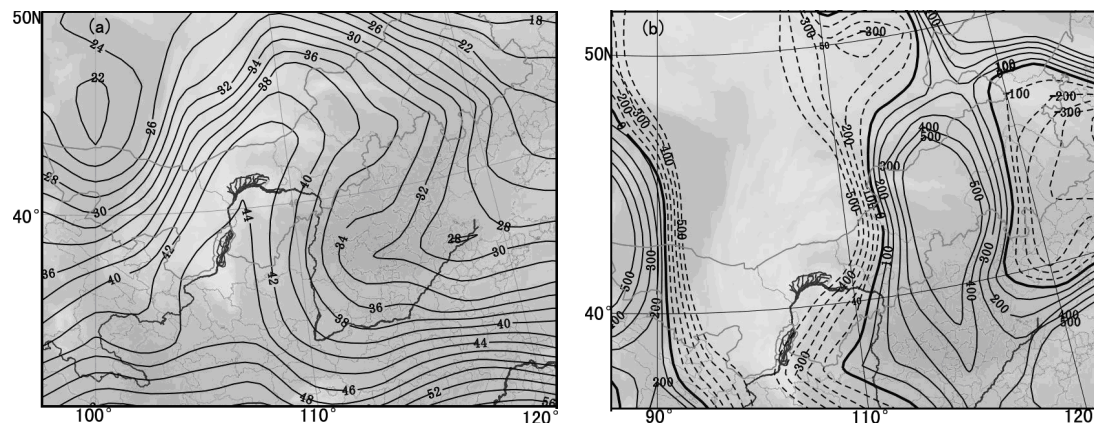


Figure 2: Superposition of water vapor image with 850hPa pseudo equivalent potential temperature (a) (unit: °C) and 700hPa vertical velocity (b) (unit: $hPa \cdot s^{-1}$) at 08:00 on the 16th

Water vapor is a tracer of atmospheric motion^[1-3], and water vapor images can better reflect the atmospheric circulation and vertical motion of its layer. Therefore, the dynamic characteristics of the water vapor belt can be analyzed through vertical motion, vorticity, and divergence^[4-6]. According to the superposition of the water vapor image and the 700hPa vertical velocity at 08:00 on April 16th (Figure 2b), it can be seen that there is a significant vertical upward movement within the water vapor belt during this precipitation process, and the position of the cloud belt corresponds well to the vertical velocity upward movement area.

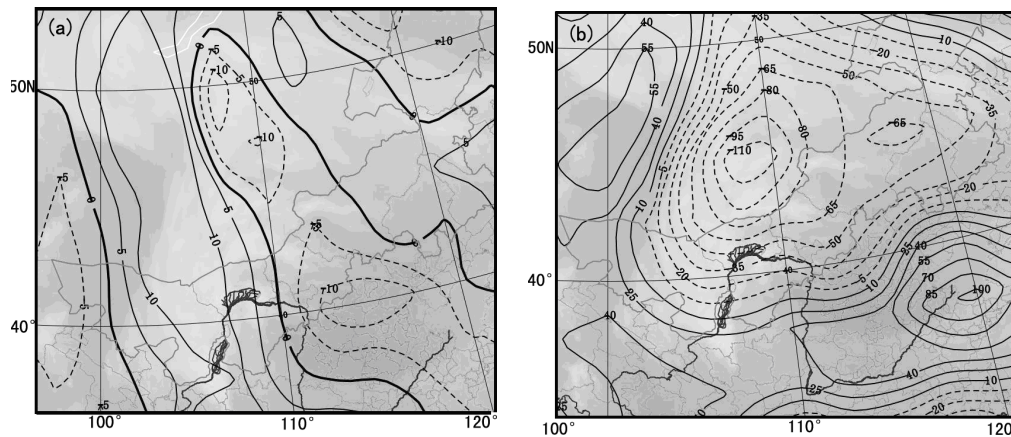


Figure 3: Superposition of water vapor image with 200hPa divergence (a) (unit: $10^{-5} s^{-1}$) and 200hPa vorticity (b) (unit: $10^{-5} s^{-1}$) at 08:00 on April 16.

From the superposition of divergence and vorticity with water vapor images at 08:00 on April 16th (Figure 3), it can be seen that the water vapor belt corresponds to the positive divergence and negative vorticity regions. The western boundary of the water vapor belt is nearly parallel to the negative vorticity belt in the upper troposphere, and a strong positive vorticity belt appears in the dark area. The distribution of divergence and vorticity at 200hPa and vertical velocity at 700hPa indicates a large-scale upward movement in the area where the water vapor belt is located.

3.2. Characteristics of dry areas

Numerous studies have shown that dry intrusion activities have a significant impact on precipitation, manifested in medium to nearly black grayscale on water vapor images. Water vapor images are effective tools for monitoring dry intrusion. From the superposition of 300hPa relative humidity $\leq 50\%$ (representing the activity of dry and cold air), positive vorticity, and wind field at 08:00 on the 16th (Figure 4), it can be seen that southwest airflow is prevalent in the dry area, and due to its influence, the dry area invades towards the northeast direction. The position of the dry zone is close to coinciding with the positive vorticity band at 300hPa. The positive vorticity center at the upper level indicates strong convergence and subsidence at the upper level of the dark region, and the positive vorticity center is transported from the upper level to the lower level (figure omitted). As the dark area weakens and disappears, precipitation tends to end, which may be related to the interruption of downdraft caused by dry intrusion [7-9]. It can be seen that moderate dry intrusion is very beneficial for the generation of precipitation.

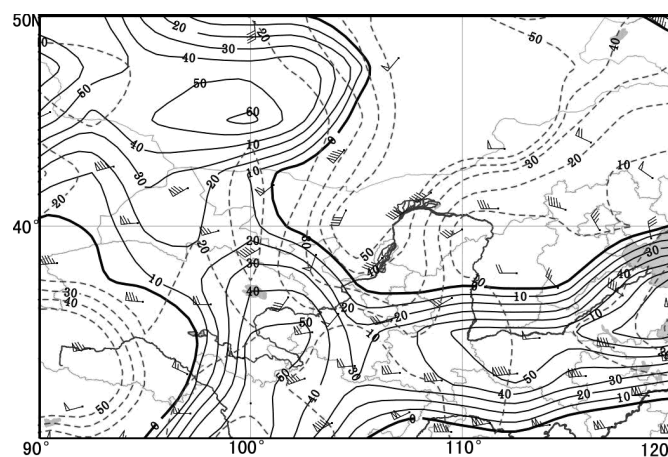


Figure 4.16 Overlay diagram of wind field with relative humidity $\leq 50\%$ (dashed line) and positive vorticity (solid line) (unit: $10^{-5} s^{-1}$) at 08:00 on the 16th at 300hPa

4. Conclusion

- (1) During this precipitation process, there is a rise. The shape and range of the ridge axis are

basically consistent with those of the water vapor belt. The area where the water vapor belt is located is a deep wet zone, with lower layers having higher levels. The maintenance of the ridge axis indicates that warm and humid airflow from low latitudes appears below the water vapor belt, which is conducive to the instability of atmospheric stratification. Due to the presence of dry intrusion in the middle and upper troposphere, it is 5-10°C higher than the outside.

(2) During this precipitation process, there was a significant vertical upward movement within the water vapor belt, and the position of the cloud belt corresponded well with the positive divergence, negative vorticity, and vertical velocity upward movement areas. The western boundary and the negative vorticity belt in the upper troposphere were nearly parallel, and a strong positive vorticity belt appeared in the position of the dark area.

(3) The position of the dry area is close to coinciding with the positive vorticity band at 300hPa, and the positive vorticity center at the upper level indicates a strong convergence and subsidence at the upper level of the dark area, and the positive vorticity center is transported from the upper level to the lower level. As the dark area weakens and disappears, precipitation tends to end, which may be related to the interruption of the downdraft caused by the invasion of the dry area.

References

- [1] Hou Qing, Xu Jianmin. 2006. *The relationship between the upper troposphere circulation pattern revealed by satellite guided wind data and the main summer rain bands in China. Journal of Applied Meteorology*, 17 (2): 138-144.
- [2] Xu Jianmin, Fang Zongyi. 2008. *Application of Satellite Water Vapor Images and Potential Vorticity Fields in Weather Analysis and Forecasting. Introduction. Meteorology*, 34 (5): 38
- [3] Bud, Forbes, J.R. Grant, et al. 1998, *Application of satellite and radar images in weather forecasting. Translated by Lu Naimang, Ran Maonong, Gu Songyan. Beijing: Science Press*, 12-82.
- [4] Cao Lixia, Zhao Liang, Xu Huaigang, et al. 2013. *Study on Water Vapor Image Interpretation of the heavy rainstorm over the Yangtze Huaihe River on July 9-10, 2007. Meteorology*, 39 (5): 605-608.
- [5] Yu Yubin, Yao Xiuping. 2003. *Research and Application Progress of Dry Invasion. Journal of Meteorology*, 61 (6): 769-778.
- [6] Yang Guiming, Mao Dongyan, Yao Xiuping. 2006. *Analysis of the dry intrusion characteristics of a Huanghuai cyclone during the Meiyu period. Journal of Tropical Meteorology*, 22(2): 176-183.
- [7] Jin Ronghua, Li Weijing, Zhang Bo, et al. 2012. *Study on the Relationship between the Activities of the East Asian Subtropical Westerly Jet and the Abnormal Meiyu in the Middle and Lower Reaches of the Yangtze River. Atmospheric Science*, 36 (4): 722-732.
- [8] Zheng Xinjiang, Lu Naimang, Luo Jingning, et al. 1997. "96.8.8" *Water vapor image feature analysis of disastrous rainstorm in Fujian. Ocean Forecast*, 14 (4): 51-58.
- [9] Wu Di, Yao Xiuping, and Shou Shaowen. 2010. *Analysis of the Effect of Dry Intrusion on a Northeast Cold Vortex Process. Plateau Meteorology*, 29 (5): 1208-1217.